

Precision measurement of the branching fractions of the $4p\ ^2P_{3/2}$ decay of Ca II

R. Gerritsma¹, G. Kirchmair^{1,2}, F. Zähringer^{1,2}, J. Benhelm^{1,2}, R. Blatt^{1,2}, and C. F. Roos^{1,2}

¹ Institut für Quantenoptik und Quanteninformation, Österreichische Akademie der Wissenschaften, Otto-Hittmair-Platz 1, A-6020 Innsbruck, Austria

² Institut für Experimentalphysik, Universität Innsbruck, Technikerstraße 25, A-6020 Innsbruck, Austria
 e-mail: Christian.Roos@uibk.ac.at

Received: October 15, 2008

Abstract. We perform precision measurements of the branching ratios of the $4p\ ^2P_{3/2}$ level decay of a single $^{40}\text{Ca}^+$ ion suspended in a linear Paul trap. High precision is achieved by a novel technique based on monitoring the population transfer when repeatedly pumping the ion between different internal states. The branching fractions into the $4s\ ^2S_{1/2}$, $3d\ ^2D_{5/2}$ and $3d\ ^2D_{3/2}$ levels are found to be 0.9347(3), 0.0587(2) and 0.00661(4), respectively. For the branching ratio $A(P_{3/2}-S_{1/2})/\sum_J A(P_{3/2}-D_J) = 14.31(5)$, we find a forty-fold improvement in accuracy as compared to the best previous measurement.

PACS. 32.70.Cs Oscillator strengths, lifetimes, transition moments – 32.80.Xx Level crossing and optical pumping – 37.10.Ty Ion trapping

1 Introduction

A precise knowledge of the radiative properties of stellar matter [1] is crucial for matching theoretical models to observations in many domains of astrophysical research [2]. Modelling isotopic abundances or the energy transport by photons in a star or a gas, in turn, requires a precise knowledge of atomic transition frequencies and oscillator strengths based on atomic structure calculations and experiments with a wide variety of neutral atoms and ions. Singly charged calcium ions have been used in various astrophysical observations [3,4]. In particular, monitoring of emission and absorption lines of dipole transitions between low-lying states has provided information about systems like galaxies [5,6], interstellar gas clouds [7], gas disks surrounding stars [8,9], and stars [10].

In laboratory experiments, cold trapped ions have received considerable attention in optical frequency metrology [11], precision measurements [12,13], and as a physical implementation of quantum information processing [14]. The ion species Ca^+ is of particular interest in this research, as it has been used for demonstrating important experimental steps in quantum information processing [15,16]. It is also studied for use in ion clocks [17,18] and for precision spectroscopy, for instance for the search of possible drifts of physical constants [19,3].

Theoretical physicists have devoted a considerable effort to improve calculations of matrix elements of transition rates and polarizabilities [20,21,22,23,24] in Ca^+ . Singly charged calcium is a quasi-hydrogenic system that

constitutes an interesting model system for testing atomic structure calculations of other singly charged alkali-earth ions with higher nuclear charge. An improved knowledge of their atomic structure would also be of interest for parity non-conservation experiments [12] in Ba^+ or Ra^+ that require precise values of transition matrix elements for a determination of the strength of parity-violating interactions. For a comparison of theoretical predictions with experimental observations, theorists often turn to precision measurements of excited state lifetimes [25,26,28,29,30,31]. Alternatively, precise measurements of branching fractions [32] of the decay of an excited state into lower-lying states could be used.

Measurements of branching ratios or oscillator strengths in ions often date back quite a long time [26] and are usually performed on ensembles of ions in discharges, ion beams [27] or trapped clouds of ions. A notable exception is a recent experiment [33] measuring the branching fractions of the $P_{3/2}$ state decay with a single trapped Ba^+ . Single trapped and laser-cooled ions form an attractive system to perform such precision measurements, as state preparation and quantum state detection can be carried out with very high fidelity. In addition, the use of single ions eliminates errors due to depolarizing collisions.

For the precision measurements reported in this paper, a single Ca^+ ion held in a linear Paul trap is employed for determining the branching fractions of the decay of the excited state $4p\ ^2P_{3/2}$ into the states $4s\ ^2S_{1/2}$, $3d\ ^2D_{5/2}$ and $3d\ ^2D_{3/2}$ (Fig. 1). We introduce a novel technique based on repetitive optical pumping to shuffle populations be-

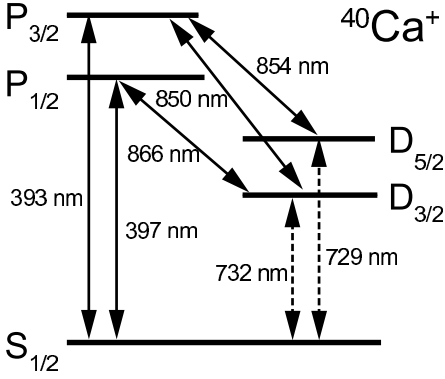


Fig. 1. Level scheme of Ca^+ showing its five lowest energy levels and the transition wavelength of the electric-dipole (solid lines) and electric-quadrupole transitions (dashed lines). The metastable D-states have a lifetime of about 1 s. In the experiments, narrow-band laser sources are available to excite all but the transition at 732 nm.

tween two of the lower-lying states. The shuffling steps are followed by detection of the population transferred to the third state. This technique surpasses the branching ratio measurement of Gallagher [26] by a factor of forty in precision and provides branching fractions with a precision of better than 1%. In combination with precision measurements of the excited $P_{3/2}$ state lifetime, our measurements lead to a more precise determination of the transition probabilities on the $S_{1/2}$ - $P_{3/2}$, $D_{3/2}$ - $P_{3/2}$, and $D_{5/2}$ - $P_{3/2}$ transitions.

2 Measurement method

A partial level scheme of Ca^+ showing its five lowest energy levels is depicted in Fig. 1. The $P_{3/2}$ state decays into the three states $S_{1/2}$, $D_{3/2}$, and $D_{5/2}$, the D-states being metastable with a lifetime of about 1.2 s [30,31]. The branching fractions p_j , i. e. the relative strengths of the decay processes, will be labelled by j , j being the angular momentum quantum number of the state into which the ion decays ($j \in \{\frac{1}{2}, \frac{3}{2}, \frac{5}{2}\}$). By definition, p_j fulfil the normalization condition $p_{1/2} + p_{3/2} + p_{5/2} = 1$. In this situation, a branching ratio is conveniently measured by (i) preparing the ion in one of the lower states, (ii) optically pumping it via the $P_{3/2}$ to the other two states, and (iii) detecting the state populations in these states [33]. This scheme is illustrated by Fig. 2(a). An ion, initially in $S_{1/2}$, is prepared in $D_{3/2}$ by optical pumping with light at 397 nm (step 1). Then, the state is completely emptied by a pulse of light at 850 nm exciting the ion to the $P_{3/2}$ state so that the ion decays into either of the states $S_{1/2}$ and $D_{5/2}$ (step 2). Finally, a quantum state measurement reveals the state into which the ion decayed. By repeating this elementary sequence M times and averaging over the measurement outcomes, an estimate \hat{r} of the decay

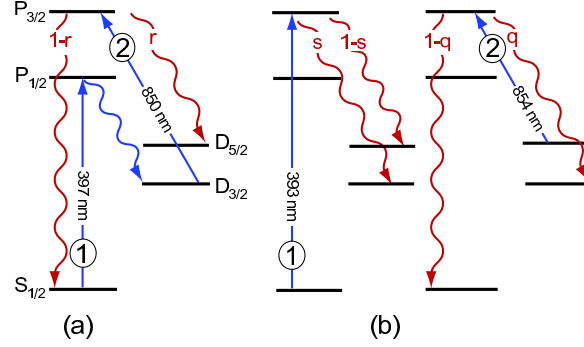


Fig. 2. Scheme for measuring the branching fractions of the $P_{3/2}$ state's decay. (a) To determine the branching ratio r between decay to the $S_{1/2}$ and $D_{5/2}$ states, we first shelve the population in the $D_{3/2}$ state by a 397 nm laser pulse (step 1). Next we empty the population in this state by a pulse of 850 nm light (step 2). After N of these cycles we measure the population in the $D_{5/2}$ state by fluorescence detection. (b) To measure another branching ratio, we first apply a pulse of 393 nm light, to populate the D-manifold via the $P_{3/2}$ state (step 1). Next we perform N cycles consisting of a pulse of 854 nm light to empty the population in the $D_{5/2}$ (step 2), followed again by a pulse of 393 nm light (step 1). Again, after N such cycles, a fluorescence measurements detects the population in the $D_{5/2}$ state. The combination of measurements (a) and (b) provides enough information to unambiguously determine the branching fractions p_j .

probability into $D_{5/2}$

$$r = p_{5/2} / (p_{1/2} + p_{5/2})$$

is obtained with a statistical error $\sigma_{\hat{r}} = \sqrt{r(1-r)/M}$ set by quantum projection noise. Note that in this measurement the branching fraction $p_{5/2}$ is normalized by the factor $p_{1/2} + p_{5/2}$ to account for the fact that population decaying back into $D_{3/2}$ is immediately pumped back by the 850 nm laser pulse. In Ca^+ , earlier experiments [26] had shown that the likelihood of a decay into $D_{5/2}$ was rather small ($r \approx 0.05$). For $r \ll 1$, the accuracy of the measurement is improved by repeating steps 1 and 2 many times before performing the state measurement. In this way, population is shuffled back and forth between $S_{1/2}$ and $D_{3/2}$, with a growing fraction accumulating in $D_{5/2}$. The population in this state after applying N cycles is given by

$$r_N = 1 - (1 - r)^N. \quad (1)$$

Resolving this equation for r yields an estimate $\hat{r} = 1 - \sqrt[N]{1 - r_N}$ for the decay probability. A short calculation shows that the uncertainty of \hat{r} can be expressed as

$$\sigma_{\hat{r}}(N) = \frac{1 - \hat{r}}{\sqrt{MN}} \sqrt{(1 - \hat{r})^{-N} - 1}, \quad (2)$$

where it was assumed that the measurement of r_N is quantum-limited in precision. Minimization of $\sigma_{\hat{r}}$ as a function of N results in the optimum number of cycles

given by

$$N^* = \frac{x^*}{-\log(1-r)}, \quad (3)$$

with the constant $x^* \approx 1.594$ minimizing the function $f(x) = \sqrt{e^x - 1}/x$. For the optimum number of measurements N^* , we have $r_N(N^*) = 1 - e^{-x^*} \approx 0.8$ and the measurement uncertainty is reduced compared to the single-cycle experiment by

$$\frac{\sigma_{\hat{r}}(N^*)}{\sigma_{\hat{r}}(N=1)} = -\sqrt{\frac{1-r}{r}} \log(1-r) f(x^*) \approx 1.24\sqrt{r},$$

the approximation being valid in the case $r \ll 1$. For $r = 0.05$, the optimum cycle number is given by $N^* = 31$. The reduction in the number of measurements needed to reach a certain level of precision directly translates into a reduction of overall measurement time as the duration of a single experiment is dominated by the time required for cooling the ion and measuring its quantum state.

A second type of experiment detecting another branching ratio is needed for determining the branching fractions p_j . Towards this end, the scheme shown in Fig. 2(b) is employed: An ion in state $S_{1/2}$ is excited to the $P_{3/2}$ state and subsequently decays into states $D_{3/2}$ and $D_{5/2}$ (step 1). Afterwards, measurement of the $D_{5/2}$ state population reveals the probability

$$s = p_{3/2}/(p_{5/2} + p_{3/2})$$

of a decay into $D_{3/2}$.

Again, the measurement accuracy can be increased by shuffling population between the states $S_{1/2}$ and $D_{5/2}$. For this, in a second step, the $D_{5/2}$ state is emptied by light at 854 nm. In this step the probability of decay into $D_{3/2}$ is given by

$$q = p_{3/2}/(p_{1/2} + p_{3/2}).$$

Now, the measurement prescription is to perform step 1, followed by N cycles consisting of step 2 and step 1, and to measure the $D_{5/2}$ state population given by

$$s_N = (1-s) \{(1-q)(1-s)\}^N. \quad (4)$$

In combination with the normalization condition $\sum_k p_k = 1$, the two measurements are sufficient for unambiguously determining the branching fractions p_j .

3 Setup

In the following, a description of the experimental setup will be given. A more detailed account can be found in ref. [16]. A single $^{40}\text{Ca}^+$ ion is trapped in a linear Paul trap with trap frequencies of 1.24 MHz and 3 MHz in the axial and radial direction, respectively. The ion is Doppler-cooled by light at 397 nm on the $S_{1/2} \leftrightarrow P_{1/2}$ transition. Light at 866 nm repumps the population lost to the $D_{3/2}$ state back into the cooling cycle. To prevent coherent population trapping in superpositions of Zeeman

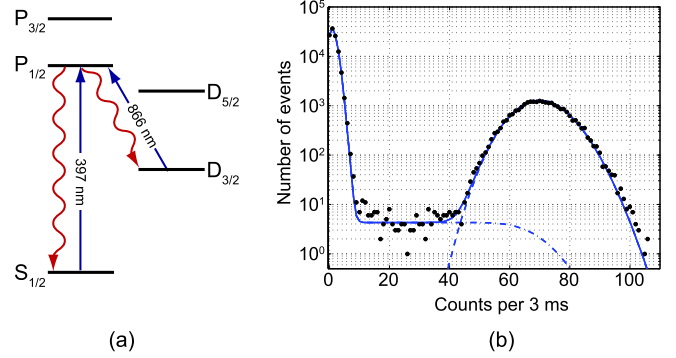


Fig. 3. Quantum state detection in Ca^+ . (a) The ion is excited by laser light on the $S_{1/2} \leftrightarrow P_{1/2}$ and $D_{3/2} \leftrightarrow P_{1/2}$ transitions for a few milliseconds. Fluorescence will be detected if the ion is in either the $S_{1/2}$ or $D_{3/2}$ state. An ion in the $D_{5/2}$ state will not fluoresce. To achieve an efficient quantum state detection, the fluorescence detection needs to be short compared to the lifetime of the metastable $D_{5/2}$ state but long enough to provide a clear separation between the photon count distributions of the ‘dark’ and the ‘bright’ states. (b) Photon count distribution constructed from 10^5 experiments. In the bright state to the right, the ion scatters on average 70 photons detected by the photomultiplier within the detection time of 3 ms. In the dark state to the left, on average 1.4 background photons are detected due to scattering of laser light from the trap electrodes. From the fit, we infer that the ion was in the $D_{5/2}$ with a probability of 0.803(1).

states, a magnetic field of about 3 G is applied to lift the degeneracy of the Zeeman states.

Commercially available diode lasers are used for generating narrow-band laser light at wavelengths of 850 nm, 854 nm and 866 nm. Laser light at 393 nm and 397 nm is derived from frequency doubled diode lasers emitting at 793 nm and 786 nm, respectively. Furthermore, a titanium sapphire laser locked to a high finesse cavity and operating at a wavelength of 729 nm is available for coherent excitation of the $S_{1/2} \leftrightarrow D_{5/2}$ transition.

The fluorescence of the ion emitted on the $S_{1/2} \leftrightarrow P_{1/2}$ transition is detected on an electron-multiplying CCD camera and a photomultiplier. For quantum state detection, the ion is excited on the $S_{1/2} \leftrightarrow P_{1/2}$ transition and the fluorescence light is collected on a photo multiplier for 3–5 ms. An average photon count rate of 23 kcounts/s is recorded when the ion is in either of the ‘bright’ $S_{1/2}$ and $D_{3/2}$ states. If the ion is in the ‘dark’ $D_{5/2}$ state, an average of 0.5 kcounts/s is detected, caused by scattering of the laser off the trap electrodes. This scheme allows for a discrimination between the quantum states with near-unit detection efficiency. The detected photon counts per measurement have a Poissonian distribution around the average value, as shown in Fig. 3. When the ion is in the $D_{5/2}$ -state however, the distribution is slightly modified due to the possibility of spontaneous decay during the detection interval. As a consequence, the Poisson distribution acquires a long tail towards the average value of counts for the S-state. To determine the probability of be-

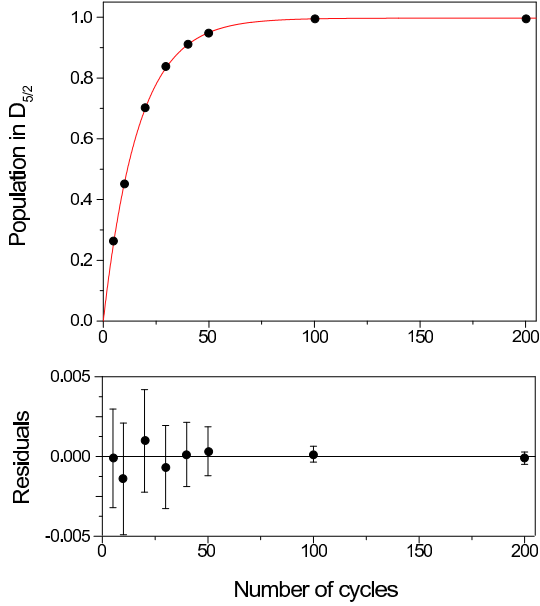


Fig. 4. Population in the $D_{5/2}$ state as a function of the number of cycles N as depicted in Fig. 2(a). Every data point consists of at least 2×10^4 measurements to determine the average population in $D_{5/2}$. The data points are jointly fitted with the measurement results presented in Fig. 5 to obtain the branching fractions p_j as described in the main text. The fitted curve is given by eq. (5). The lower plot shows the residuals with errors bars given by the statistical uncertainty due to the finite number of measurements.

ing in the bright or dark state at the end of an experiment, we repeat the experiment M times and record the resulting photon counts. Then, a maximum likelihood method is used to determine the probability p for the ion of being in the dark state. For each single experiment, we compute the probability of observing the detected number of photon counts given p and multiply these probabilities for all experiments to obtain an overall probability Π . The probability p_D determined by the maximum likelihood estimate then corresponds to the value of p that maximizes the probability Π .

In order to discriminate between the $S_{1/2}$ and the $D_{3/2}$ state, the $S_{1/2}$ state population is coherently transferred to the $D_{5/2}$ state prior to state detection by a laser exciting the $S_{1/2} \leftrightarrow D_{5/2}$ quadrupole transition. For this, either resonant laser π -pulses or rapid adiabatic passages [34] are used connecting pairs of Zeeman states in the ground and the metastable state. This way, we achieve a transfer probability of better than 99.5%.

4 Measurement results

For the experimental determination of the $P_{3/2}$ state's branching fractions, a single ion is loaded into the trap. The first experiment implements the scheme depicted in Fig. 2(a). We start by measuring the time it takes to completely empty the $S_{1/2}$ state by light at 397 nm. For this, a laser pulse of variable length is applied to an ion prepared

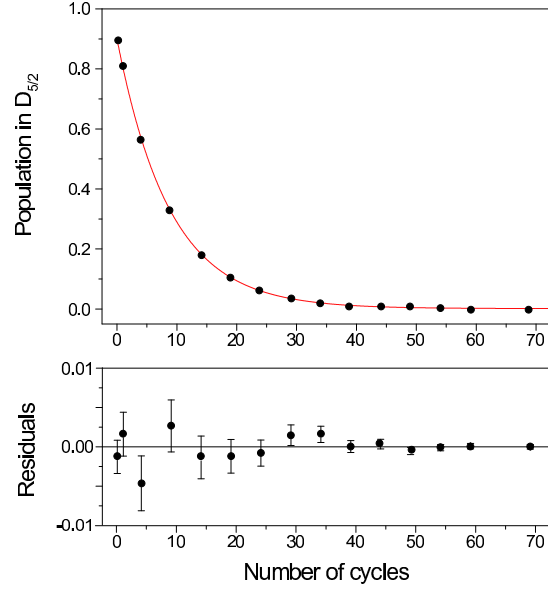


Fig. 5. Population in the $D_{5/2}$ state as a function of the number of cycles N as depicted in Fig. 2(b). The lower plot shows the residuals after fitting the data. The fitted curve is given by eq. (6).

in state $S_{1/2}$, and subsequently the population transferred to the $D_{3/2}$ state is detected by shelving the remaining $S_{1/2}$ state population in the $D_{5/2}$ level. Fitting an exponentially decaying function to the $S_{1/2}$ state population, we find a $1/e$ time of $1\ \mu\text{s}$. In a similar measurement, we determined the decay time of population in $D_{3/2}$ to be $16\ \mu\text{s}$ when emptying the state by light at 850 nm. In a next step, we implement a population shuffling cycle by switching on the laser at 397 nm for $20\ \mu\text{s}$ before turning on the laser at 850 nm for a duration of $100\ \mu\text{s}$. We repeat this cycle N times to slowly accumulate all the population in the $D_{5/2}$ state. Fig. 4 shows the $D_{5/2}$ state population for cycle numbers ranging from 5 to 200 by repeating the experiment for each value of N between 20000 and 23000 times. The experimental results are fitted by slightly modifying eq. (1) to

$$r_{N,exp} = A(1 - (1 - r)^N) \quad (5)$$

by introducing a scaling factor A to account for the fact that even after 200 pumping cycles the measurement finds 0.3% of the population to be outside the $D_{5/2}$ state. This effect is caused by the finite lifetime of the metastable states as will be discussed in subsection 5.2.

A similar procedure is applied for implementing the scheme depicted in Fig. 2(b). The $1/e$ pumping times for emptying the states $S_{1/2}$ and $D_{5/2}$ by light at 393 nm and 854 nm are determined to be $2\ \mu\text{s}$ each. Based on this measurement, a pumping cycle - transferring population from $D_{5/2}$ to $S_{1/2}$ and back again - was chosen that consisted of a laser pulse at 854 nm of $20\ \mu\text{s}$ duration, followed by another $20\ \mu\text{s}$ pulse at 393 nm. Again, we measure the population remaining in the $D_{5/2}$ state after N pumping cycles, N varying between 0 and 69. Fig. 5 shows the experimental results obtained by repeating the experiment

20000 times for each value of N . We fit the results by modifying eq. (4) to

$$s_{N,exp} = (1 - s) \{(1 - q)(1 - s)\}^N + B. \quad (6)$$

Here, the offset B accounts for 0.03% of the population seemingly remaining in the $D_{5/2}$ state. The error bars appearing in Fig. 4 and Fig. 5 are of statistical nature due to the finite number N of experiments.

The parameters r , s , q appearing in equations (5) and (6) can be expressed by $p_{3/2}$ and $p_{5/2}$. To determine the branching fractions p_j , we use a weighted least-square fit to jointly fit both decay curves by the set of parameter $\{p_{3/2}, p_{5/2}, A, B\}$, assuming that the measurement error is given by quantum projection noise. With this procedure, we find $p_{1/2} = 0.9347(3)$, $p_{3/2} = 0.00661(4)$, $p_{5/2} = 0.0587(2)$, and $A = 0.9971(3)$, $B = 0.0013(2)$. The error bars are obtained from a Monte-Carlo bootstrapping technique [35]. We randomly vary the experimentally observed $D_{5/2}$ populations p by shifting their values assuming a Gaussian distribution with variance $p(1 - p)/M$ and fit the resulting data set. Repeating this procedure 1000 times, the spread of the simulated fit parameters provides us with an error estimate for the branching fractions.

5 Discussion

5.1 Statistical errors

In the regression analysis used for determining the branching fractions, we assume the errors to be quantum-noise limited. This means that we consider the outcome of an individual experiment to be given by a random variable X_i , $i = 1, \dots, M$, yielding the outcome ‘1’ with probability p and the outcome ‘0’ with probability $1 - p$. For a set of M experiments, we then assume the standard deviation of $X = \frac{1}{M} \sum_{i=1}^M X_i$ to be given by $\sigma_p = \sqrt{p(1 - p)/M}$. If, however, due to experimental imperfections the probability p slightly changes over the course of time needed for carrying out the M experiments, this assumption would be violated. We therefore checked the validity of our hypothesis by subdividing our data into K sets S_k , $k = 1, \dots, K$, each containing M/K consecutively taken experiments described by the random variables $\{X_{j_k+1}, \dots, X_{j_k+M/K}\}$. For each set S_k , we compute its mean value $p^{(k)} = \frac{K}{M} \sum_{i \in S_k} \langle X_i \rangle$ and its deviation $p^{(k)} - p$ from the average probability. We repeat this procedure for different values of K ranging from 2 to 1000. A comparison of the distribution of $p^{(k)} - p$ with the one expected for truly random variable all having the same probability p leads us to conclude that the assumption of quantum-limited errors is well-justified.

5.2 Systematic errors

The method of measuring the branching fractions by repeated optical pumping assumes that the optical pumping steps are perfect. If, however, a small fraction $\epsilon_{1,2}$ is not

pumped out in the two pumping steps of the cycle, the measured decay rates will be smaller than for perfect optical pumping. This systematic effect is taken into account by defining an effective cycle number $N_{eff} = N(1 - \epsilon_1 - \epsilon_2)$ that replaces the cycle number N in equations (5) and (6). This correction was actually applied in the data evaluation of the first experiment as it turned out that the laser pulse at 850 nm of 100 μ s duration was too short to completely empty the $D_{3/2}$ state ($\epsilon_2 = 0.3\%$ of the population were left behind).

The finite lifetime $\tau_D = 1.2$ s of the metastable D-states also has a small effect on the measured branching ratios. The quantum state detection method we use is not affected by spontaneous decay processes occurring during the detection time. Spontaneous decay during the pumping cycle, however, slightly modifies the results. This is best illustrated by the pumping scheme shown in Fig. 2(a). Spontaneous decay of the $D_{3/2}$ state is negligible since the state is emptied by light at 850 nm in 16 μ s, i.e. with a rate roughly 10^4 times bigger than the spontaneous decay rate. The situation is different for the $D_{5/2}$ state which is populated by a rate $R_a = r\tau_{cycle}^{-1}$ where $\tau_{cycle} = 120$ μ s is the duration of a single pumping cycle. Here, spontaneous decay gives rise to a steady-state $D_{5/2}$ state population $p_{D,\infty} = 1 - R_a\tau_D \approx 99.8\%$ in the limit of an infinite number of pumping cycles which is consistent with the measured value of the fit multiplier A . In addition to changing the steady state solution, the additional decay process also decreases the time required for reaching the equilibrium (see eq. (5)). This effect was taken into account in the analysis of the branching fractions stated in Tab. 1.

A similar argument can be made for spontaneous decay affecting the pumping scheme of Fig. 2(b). Here, the $D_{3/2}$ is populated with a rate $R_b \approx s\tau_{cycle}^{-1}$ which needs to be compared to the spontaneous decay rate $1/\tau_D$. Due to this effect, we expect to find a steady-state population of about 0.04% that is not in $D_{3/2}$. Here, the effect is smaller since $r < s$ and the duration of the pumping cycle was about five times shorter than in the other experiment. The correction to the measured rate is also about 0.04% and does not significantly alter our measurement. Before performing the branching ratio measurements, we had checked that the lifetimes of the metastable states were not significantly shortened by the lasers at 850 and 854 nm which could occur either by a broad-band frequency background of the diode lasers producing the light or by imperfectly switched off laser beams.

In general, any additional mechanism that leads to an exchange of population between the atomic states will modify the steady-state population obtained in the limit of large N and shorten the time scale required for reaching the steady-state. Spin-changing collisions leading to transitions between the $D_{3/2}$ and the $D_{5/2}$ state are of no importance in our measurements as they occur at a rate that is smaller than $10^{-2}s^{-1}$.

Table 1. Branching fractions of the decay of the $P_{3/2}$ state as found in the present work compared to various theoretical values from the literature. Ref. [22] gives the relative decay strengths of the state $4p$ into $4s$ and $3d$. The last two columns give the Einstein coefficients A_{fi} measured from the branching fractions in combination with the lifetime measurement of ref. [29] and the theoretical prediction of ref. [23].

Transition	Branching fractions					$A_{fi} \times 10^6 s^{-1}$	
	Present work	ref. [20]	ref. [21]	ref. [22]	ref. [23]	Present work+[29]	ref. [23]
$4P_{3/2} \leftrightarrow 4S_{1/2}$	0.9347(3)	0.9381	0.9354	0.9357	0.9340	135.0(4)	139.7
$4P_{3/2} \leftrightarrow 3D_{3/2}$	0.00661(4)	0.00628	0.00649	0.0643	0.00667	0.955(6)	0.997
$4P_{3/2} \leftrightarrow 3D_{5/2}$	0.0587(2)	0.0556	0.0581		0.0593	8.48(4)	8.877

5.3 Comparison with other measurements and calculations

The branching fractions obtained from fitting the two decay measurement can be compared to previous measurements and theoretical calculations. By evaluating the ratio $p_{3/2}/(p_{1/2} + p_{5/2})$, we find $A_{(P_{3/2}-S_{1/2})}/\sum_J A_{(P_{3/2}-D_J)} = 14.31(5)$ for the branching ratio of the decay into the S- and D-states. This is a bit lower than the value of 17.6(2.0) measured by Gallagher [26] in a discharge experiment in 1967. A comparison with theoretical calculations [20,21, 22,23] is given in Tab. 1, showing a good agreement between experiment and theory.

When combining the branching ratio measurements with an experimental determination [29] of the $P_{3/2}$ state's lifetime, the relative decay strengths can be converted into Einstein A coefficients which are also given in Tab. 1. We also list the theoretical predictions of ref. [23] which are all about 4% higher, a discrepancy much bigger than for the relative decay strengths. From this point of view, it might be of interest to use a single trapped ion for a measurement of its excited state lifetime [36] or its absolute oscillator strengths.

5.4 Measuring Einstein coefficients in a single ion

A large variety of methods exists for measuring transition matrix elements in ensembles of neutral atoms or ions [32]. In view of the discrepancy between the Einstein coefficients calculated from experimental observations and predicted by theory, we would like to propose yet another technique capable of directly measuring Einstein coefficients in a single ion. We will discuss the technique for the case of the decay rate of the $P_{1/2} \leftrightarrow D_{3/2}$ transition.

We start with an ion initially prepared in the $S_{1/2}$ state. A narrow-band laser off-resonantly exciting the $S_{1/2} \leftrightarrow P_{1/2}$ transition pumps the ion into the $D_{3/2}$ state. If the detuning Δ of the laser is much bigger than the inverse of the excited state lifetime, the pumping rate is given by $R = A_{(P_{1/2}-D_{3/2})}\rho_{P_{1/2}}$ where $\rho_{P_{1/2}} = \Omega^2/(4\Delta^2)$ is the excited state population and Ω the Rabi frequency of the laser exciting the transition. The Rabi frequency is related to the ac-Stark shift $\delta_{ac} = \Omega^2/(4|\Delta|)$ experienced by the $S_{1/2}$ state due to the presence of the off-resonant light. In this way, the Einstein coefficient can be expressed

by

$$A_{(P_{1/2}-D_{3/2})} = R \frac{\Delta}{\delta_{ac}}.$$

A measurement of the pumping rate could be performed in a similar way as the experiments presented in this paper by shelving the $S_{1/2}$ population in $D_{5/2}$ prior to quantum state detection. For the determination of the light shift δ_{ac} , a spin echo experiment could be performed on the $S_{1/2} \leftrightarrow D_{5/2}$ transition, measuring the shift of the transition frequency by the light pumping the ion. Measurements of this type have recently been shown [37] to be able to resolve level shifts as small as 1 Hz. To give an example, we assume $\Delta = (2\pi) 10^{10} s^{-1}$ and adjust the Rabi frequency to get $R = 10^2 s^{-1}$. Because of $A_{(P_{1/2}-D_{3/2})} \approx 10^7 s^{-1}$, the light shift will be $\delta_{ac} = (2\pi) 10^5 s^{-1}$. To measure the Einstein coefficient to better than 1% would require a measurement of the light shift with a precision of better than 1 kHz within a measurement time somewhat shorter than $1/R = 10$ ms which appears to be feasible.

For a proper treatment, the Zeeman sublevels of the atomic levels need to be taken into account. Fortunately, in the case of the $S_{1/2} \leftrightarrow P_{1/2}$ transition, the pumping rate and the induced light shift are independent of the polarization of the exciting laser as long as it is linearly polarized. In this way, the Einstein coefficient could be independently measured with high precision to complement the branching ratio measurements presented in this paper.

5.5 Conclusion

Our experiments demonstrate that single trapped ions are perfectly suited for a precision measurement of branching fractions. As compared to experiments based on a single pumping step, the technique of repeated optical pumping offers two important advantages. Firstly, it reduces the number of measurements required for obtaining a given level of accuracy in the case where the transition probabilities to the lower-lying states are very different. Secondly, monitoring the population transfer as a function of the number of the pumping cycle provides a means to detect possible sources of errors like atomic state changes induced by sources other than the lasers used for optical pumping.

The pumping technique used in this paper requires an atom with a tripod level structure, i. e. an upper state decaying into three lower-lying states. As this level structure

exists not only in Ca^+ but also in many other isotopes, the method should be widely applicable.

We gratefully acknowledge the support of the European network SCALA, the Institut für Quanteninformation GmbH and IARPA. R. G. acknowledges funding of the Marie-Curie program of the European Union (grant number PIEF-GA-2008-220105). C. F. R. would like to thank J. Mitroy and M. Safronova for useful discussions.

References

1. M. J. Seaton, Y. Yan, D. Mihalas, A. K. Pradhan, *Mon. Not. R. Astron. Soc.* **266**, 805 (1994).
2. F. J. Rogers, C. A. Iglesias, *Science* **263**, 50 (1994).
3. A. L. Wolf, S. A. van den Berg, C. Gohle, E. J. Salumbides, W. Ubachs, K. S. E. Eikema, *Phys. Rev. A* **78**, 032511 (2008).
4. E. Biémont, C. J. Zeippen, *Comments At. Mol. Phys.* **33**, 29 (1996).
5. S. E. Persson, *Astrophys. J.* **330**, 751 (1988).
6. C. H. Nelson, M. Whittle, *Astrophys. J. Suppl. Ser.* **99**, 67 (1995).
7. D. E. Welty, D. C. Morton, L. M. Hobbs, *Astrophys. J. Suppl. Ser.* **106**, 533 (1996).
8. R. Ferlet, L. M. Hobbs, A. Vidal-Madjar, *Astron. Astrophys.* **185**, 267 (1987).
9. L. M. Hobbs, A. M. Lagrange-Henri, R. Ferlet, A. Vidal-Madjar, D. E. Welty, *Astrophys. J.* **334**, L41 (1988).
10. L. Mashonkina, A. J. Korn, N. Przybilla, *Astron. Astrophys.* **461**, 261 (2007).
11. S. A. Diddams *et al.*, *Science* **293**, 825 (2001).
12. N. Fortson, *Phys. Rev. Lett.* **70**, 2383 (1993).
13. H. Häffner *et al.*, *Phys. Rev. Lett.* **85**, 5308 (2000).
14. J. I. Cirac, P. Zoller, *Phys. Rev. Lett.* **74**, 4091 (1995).
15. M. Riebe *et al.*, *Nature* **429**, 734 (2004).
16. J. Benhelm, G. Kirchmair, C. F. Roos, R. Blatt, *Nature Physics* **4**, 463 (2008).
17. C. Champenois, M. Houssin, C. Lisowski, M. Knoop, G. Hagel, M. Vedel, F. Vedel, *Phys. Lett. A* **331**, 298 (2004).
18. M. Chwalla *et al.*, arXiv:0806.1414 (2008).
19. V. A. Dzuba, V. V. Flambaum, J. K. Webb, *Phys. Rev. A* **59**, 230 (1999).
20. C. Guet, W. R. Johnson, *Phys. Rev. A* **44**, 1531 (1991).
21. S.-S. Liaw, *Phys. Rev. A* **51**, R1723 (1995).
22. J. Mitroy, J. Y. Zhang, *Eur. Phys. J. D* **46**, 415 (2007).
23. B. Arora, M. S. Safronova and C. W. Clark, *Phys. Rev. A* **76**, 064501 (2007).
24. B. K. Sahoo, *Chem. Phys. Lett.* **448**, 144 (2007).
25. W. W. Smith, A. Gallagher, *Phys. Rev.* **145**, 26 (1966).
26. Alan Gallagher, *Phys. Rev.* **157**, 24 (1967).
27. S. G. Cox, A. D. J. Critchley, I. R. McNab, F. E. Smith *Meas. Sci. Technol.* **10**, R101 (1999).
28. R. N. Gosselin, E. H. Pinnington, W. Ansbacher, *Phys. Rev. A* **38**, 4887 (1988).
29. J. Jin, D. A. Church, *Phys. Rev. Lett.* **70**, 3213 (1993).
30. P. A. Barton, C. J. S. Donald, D. M. Lucas, D. A. Stevens, A. M. Steane, D. N. Stacey, *Phys. Rev. A* **62**, 032503 (2000).
31. A. Kreuter *et al.*, *Phys. Rev. A* **71**, 032504 (2005).
32. M. C. E. Huber, R. J. Sandeman, *Rep. Prog. Phys.* **49**, 397 (1986).
33. N. Kurz, M. R. Dietrich, Gang Shu, R. Bowler, J. Salacka, V. Mirgon, B. B. Blinov, *Phys. Rev. A* **77**, 060501(R) (2008).
34. Chr. Wunderlich *et al.*, *J. Mod. Opt.* **54**, 1541 (2007).
35. B. Efron, R. Tibshirani, *Stat. Science* **1**, 54 (1986).
36. D. L. Moehring *et al.*, *Phys. Rev. A*, **73**, 023413 (2006).
37. C. F. Roos, T. Monz, K. Kim, M. Riebe, H. Häffner, D. F. V. James, R. Blatt, *Phys. Rev. A* **77**, 040302(R) (2008).